



THE UNIVERSITY *of* EDINBURGH

Edinburgh Research Explorer

Can Kozai-Lidov cycles explain Kepler-78b?

Citation for published version:

Rice, K 2015, 'Can Kozai-Lidov cycles explain Kepler-78b?' Monthly Notices of the Royal Astronomical Society, vol. 448, no. 2, pp. 1729-1737. DOI: 10.1093/mnras/stv073

Digital Object Identifier (DOI):

[10.1093/mnras/stv073](https://doi.org/10.1093/mnras/stv073)

Link:

[Link to publication record in Edinburgh Research Explorer](#)

Document Version:

Publisher's PDF, also known as Version of record

Published In:

Monthly Notices of the Royal Astronomical Society

General rights

Copyright for the publications made accessible via the Edinburgh Research Explorer is retained by the author(s) and / or other copyright owners and it is a condition of accessing these publications that users recognise and abide by the legal requirements associated with these rights.

Take down policy

The University of Edinburgh has made every reasonable effort to ensure that Edinburgh Research Explorer content complies with UK legislation. If you believe that the public display of this file breaches copyright please contact openaccess@ed.ac.uk providing details, and we will remove access to the work immediately and investigate your claim.



Can Kozai–Lidov cycles explain Kepler-78b?

Ken Rice[★]

Scottish Universities Physics Alliance (SUPA), Institute for Astronomy, University of Edinburgh, Blackford Hill, Edinburgh EH9 3HJ, UK

Accepted 2015 January 13. Received 2015 January 12; in original form 2014 October 01

ABSTRACT

Kepler-78b is one of a growing sample of planets similar, in composition and size, to the Earth. It was first detected with NASA’s *Kepler* spacecraft and then characterized in more detail using radial velocity follow-up observations. Not only is its size very similar to that of the Earth ($1.2 R_{\oplus}$), it also has a very similar density (5.6 g cm^{-2}). What makes this planet particularly interesting is that it orbits its host star every 8.5 h, giving it an orbital distance of only 0.0089 au. What we investigate here is whether or not such a planet could have been perturbed into this orbit by an outer companion on an inclined orbit. In this scenario, the outer perturber causes the inner orbit to undergo Kozai–Lidov cycles which, if the periape comes sufficiently close to the host star, can then lead to the planet being tidally circularized into a close orbit. We find that this process can indeed produce such very-close-in planets within the age of the host star ($\sim 600\text{--}900$ Myr), but it is more likely to find such ultrashort-period planets around slightly older stars (> 1 Gyr). However, given the size of the *Kepler* sample and the likely binarity, our results suggest that Kepler-78b may indeed have been perturbed into its current orbit by an outer stellar companion. The likelihood of this happening, however, is low enough that other processes – such as planet–planet scattering – could also be responsible.

Key words: planets and satellites: formation – planets and satellites: general – planet–star interactions.

1 INTRODUCTION

Analysis of data from NASA’s *Kepler* spacecraft (Borucki et al. 2010; Batalha et al. 2013) indicates that planets with radii similar to that of the Earth are common (Dressing & Charbonneau 2013; Petigura, Marcy & Howard 2013). Recently it was announced that one of the *Kepler* targets (Kepler-78) showed a 0.02 per cent decline in brightness that was associated with a planet with a radius of only $1.16 \pm 0.19 R_{\oplus}$ (Sanchis-Ojeda et al. 2013). Follow-up observations, using HARPS-N (Cosentino et al. 2012) and the High Resolution Echelle Spectrometer (Vogt et al. 1994), confirmed that this is indeed a planet with a mass of about $1.86 M_{\oplus}$ and a density of about 5.6 g cm^{-3} (Howard et al. 2013; Pepe et al. 2013).

Of course it is fascinating that we are now detecting planets with sizes and densities similar to that of the Earth, but what makes this planet particularly interesting is that it has an orbital period of only 8.5 h, meaning that it is orbiting at a distance of only 0.0089 au from its parent star. Quite how such a planet can end up in such an orbit is very uncertain. It almost certainly could not have formed where it now resides, as the temperature in the disc in that region would have been too high even for dust grains to condense (Bell

et al. 1997). It could potentially have migrated inwards through disc migration. However, such low-mass planets would migrate in the gapless, Type I regime (Ward 1997) which is typically thought to be so fast (Tanaka, Takeuchi & Ward 2002; Kley & Crida 2008) that it would seem unlikely that such objects could be left stranded so close to their parent stars. Population synthesis models (Ida & Lin 2008; Mordasini, Alibert & Benz 2009) typically assume a reduced Type I migration rate.

Alternatively, such close-in planets could be scattered on to eccentric orbits (Ford & Rasio 2006) that are then circularized through tidal interactions with the parent star (Rasio et al. 1996). It has indeed been suggested that if such a process were to operate, we should be seeing some very short period hot super-Earths (Schlaufman, Lin & Ida 2010), so this could be an explanation for the origin of Kepler-78b. However, even this study suggested that typical orbital periods would be greater than the 8.5 h orbital period of Kepler-78b.

Another mechanism for forming close-in planets, related to dynamical interactions in multiplanet systems, is for the planet to undergo Kozai–Lidov cycles driven by a stellar companion on a highly inclined orbit (Kozai 1962; Lidov 1962). If the eccentricity is sufficiently large, so that the periastron becomes very small, the planet’s orbit may be circularized through tidal interactions with its host star (Wu & Murray 2003; Fabrycky & Tremaine 2007). What

[★] E-mail: wkmr@roe.ac.uk

we want to investigate in this paper is whether or not this process could indeed explain the origin of Kepler-78b. Given that binarity amongst solar-like stars is quite high (Duquennoy & Mayor 1991; Abt & Willmarth 2006) it seems likely that this could play a role in producing close-in, Earth-sized planets.

In this paper, we present results from a series of Monte Carlo simulations in which we consider how a planet with a mass and density the same as that of Kepler-78b, but initially orbiting between 0.5 and 2 au, is influenced by perturbations from a binary stellar companion. We also include the influence of tides, which would allow the orbit to circularize if the eccentricity becomes sufficiently large, and the influence of general relativistic (GR) and apsidal precession. This paper is organized as follows : in Section 2 we present equations of motion, in Section 3 we describe the basic setup of the problem, in Section 4 we discuss the results, and in section 5 we discuss the results and draw some conclusions.

2 EQUATIONS OF MOTION

The goal is to evolve an inner binary (planet and star) under the influence of tidal interactions, perturbing accelerations from stellar and planetary distortions due to tides and rotation, perturbing accelerations from a third body, and GR apsidal precession. To quadrupole order, these equations were first presented by (Eggleton & Kiseleva 2001) and can also be found in Wu & Murray (2003) and Fabrycky & Tremaine (2007).

Rather than using the equations in Eggleton & Kiseleva (2001), we have implemented those from Barker & Ogilvie (2009) and Barker (2011) which are regular at $e = 0$. We want to evolve an inner system (planet + host star), where the bodies have masses M_s and M_p , radii R_s and R_p , and in which the orbit has an eccentricity e , semimajor axis a , and orbital angular frequency $n = \sqrt{G(M_s + M_p)/a^3}$. The vector quantities that we want to evolve are, therefore, the spin of the parent star $\boldsymbol{\Omega}_s$, the spin of the planet $\boldsymbol{\Omega}_p$, the eccentricity of the inner orbit \mathbf{e} , and angular momentum vector of the inner orbit $\mathbf{h} = \mathbf{r} \times \dot{\mathbf{r}} = na^2\sqrt{1-e^2}\hat{\mathbf{h}}$.

We have built our model by considering, initially, only the equations that evolve these quantities through tidal dissipation and a stellar wind. From Barker & Ogilvie (2009), we have

$$\begin{aligned} \frac{d\mathbf{h}}{dt} = & -\frac{1}{t_{fs}} \left[\frac{\boldsymbol{\Omega}_s \cdot \mathbf{e}}{2n} f_5(e^2) h \mathbf{e} \right. \\ & \left. - \frac{\boldsymbol{\Omega}_s}{2n} f_3(e^2) h + \left(f_4(e^2) - \frac{\boldsymbol{\Omega}_s \cdot \mathbf{h}}{2n} \frac{1}{h} f_2(e^2) \right) \mathbf{h} \right] \\ & - \frac{1}{t_{fp}} \left[\frac{\boldsymbol{\Omega}_p \cdot \mathbf{e}}{2n} f_5(e^2) h \mathbf{e} - \frac{\boldsymbol{\Omega}_p}{2n} f_3(e^2) h \right. \\ & \left. + \left(f_4(e^2) - \frac{\boldsymbol{\Omega}_p \cdot \mathbf{h}}{2n} \frac{1}{h} f_2(e^2) \right) \mathbf{h} \right] \\ = & \left(\frac{d\mathbf{h}}{dt} \right)_s + \left(\frac{d\mathbf{h}}{dt} \right)_p \end{aligned} \quad (1)$$

$$\begin{aligned} h \frac{de}{dt} = & -\frac{1}{t_{fs}} \left[\frac{\boldsymbol{\Omega}_s \cdot \mathbf{e}}{2n} f_2(e^2) h + 9 \left(f_1(e^2) h - \frac{11}{18} \frac{\boldsymbol{\Omega}_s \cdot \mathbf{h}}{n} f_2(e^2) \right) \mathbf{e} \right] \\ & - \frac{1}{t_{fp}} \left[\frac{\boldsymbol{\Omega}_p \cdot \mathbf{e}}{2n} f_2(e^2) h + 9 \left(f_1(e^2) h - \frac{11}{18} \frac{\boldsymbol{\Omega}_p \cdot \mathbf{h}}{n} f_2(e^2) \right) \mathbf{e} \right] \end{aligned} \quad (2)$$

$$\frac{d\boldsymbol{\Omega}_s}{dt} = -\frac{\mu}{I_s} \left(\frac{d\mathbf{h}}{dt} \right)_s + \dot{\boldsymbol{\Omega}}_{\text{swind}} \quad (3)$$

$$\frac{d\boldsymbol{\Omega}_p}{dt} = -\frac{\mu}{I_p} \left(\frac{d\mathbf{h}}{dt} \right)_p, \quad (4)$$

where I_s and I_p are the moments of inertia of the star and planet, $\boldsymbol{\Omega}_{\text{swind}}$ represents the stellar wind, and $\mu = M_s M_p / (M_s + M_p)$ is the reduced mass of the inner system. We also need to define the tidal friction time-scales for the star and planet (t_{fs} and t_{fp}), which depend on the star and planet's tidal quality factors (Q'_s and Q'_p), and the functions of the eccentricity.

$$\frac{1}{t_{fs}} = \left(\frac{9n}{2Q'_s} \right) \left(\frac{M_p}{M_s} \right) \left(\frac{R_s}{a} \right)^5 \quad (5)$$

$$\frac{1}{t_{fp}} = \left(\frac{9n}{2Q'_p} \right) \left(\frac{M_s}{M_p} \right) \left(\frac{R_p}{a} \right)^5 \quad (6)$$

$$f_1(e^2) = \frac{1 + \frac{15}{4}e^2 + \frac{15}{8}e^4 + \frac{5}{64}e^6}{(1-e^2)^{\frac{13}{2}}} \quad (7)$$

$$f_2(e^2) = \frac{1 + \frac{3}{2}e^2 + \frac{1}{8}e^4}{(1-e^2)^5} \quad (8)$$

$$f_3(e^2) = \frac{1 + \frac{9}{2}e^2 + \frac{5}{8}e^4}{(1-e^2)^5} \quad (9)$$

$$f_4(e^2) = \frac{1 + \frac{15}{2}e^2 + \frac{45}{8}e^4 + \frac{5}{16}e^6}{(1-e^2)^{\frac{13}{2}}} \quad (10)$$

$$f_5(e^2) = \frac{3 + \frac{1}{2}e^2}{(1-e^2)^5} \quad (11)$$

$$f_6(e^2) = \frac{1 + \frac{31}{2}e^2 + \frac{255}{8}e^4 + \frac{5}{16}e^6 + \frac{25}{64}e^8}{(1-e^2)^8}. \quad (12)$$

We also include the contributions due to an additional outer body (b) of mass M_o , orbital angular frequency n_o , semimajor axis a_o , and eccentricity e_o . Additionally, we add contributions from quadrupolar distortions of the inner star and planet due to tidal and rotational bulges (qs and qp), and we include GR apsidal precession. The equations, shown below, are taken from Barker (2011)

$$\left(\frac{d\mathbf{h}}{dt} \right)_b = -3C_b h \left[\frac{(1-e^2)}{h^2} (\mathbf{n} \cdot \mathbf{h})(\mathbf{n} \times \mathbf{h}) - 5(\mathbf{n} \cdot \mathbf{e})(\mathbf{n} \times \mathbf{e}) \right] \quad (13)$$

$$\left(\frac{d\mathbf{h}}{dt} \right)_{qs} = -\frac{\alpha_s}{h(1-e^2)^2} (\boldsymbol{\Omega}_s \cdot \mathbf{h})(\boldsymbol{\Omega}_s \times \mathbf{h})$$

$$\left(\frac{d\mathbf{h}}{dt} \right)_{qp} = -\frac{\alpha_p}{h(1-e^2)^2} (\boldsymbol{\Omega}_p \cdot \mathbf{h})(\boldsymbol{\Omega}_p \times \mathbf{h}) \quad (14)$$

$$\begin{aligned} h \left(\frac{de}{dt} \right)_b = & 3C_b (1-e^2) \left[2(\mathbf{h} \times \mathbf{e}) - (\mathbf{n} \cdot \mathbf{h})(\mathbf{n} \times \mathbf{e}) \right. \\ & \left. + 5(\mathbf{n} \cdot \mathbf{e})(\mathbf{n} \times \mathbf{h}) \right] \end{aligned} \quad (15)$$

$$\begin{aligned}
 h \left(\frac{d\mathbf{e}}{dt} \right)_{\text{qs}} &= \frac{\alpha_s}{(1-e^2)^2} \left[\frac{1}{2} \left(\frac{3}{h^2} (\boldsymbol{\Omega}_s \cdot \mathbf{h})^2 - \Omega_s^2 \right) \right. \\
 &\quad \left. + \frac{15 GM_p}{a^3} f_2(e^2)(1-e^2)^2 \right] (\mathbf{h} \times \mathbf{e}) \\
 &\quad + \frac{\alpha_s}{h^2(1-e^2)^2} (\boldsymbol{\Omega}_s \cdot \mathbf{h})(\boldsymbol{\Omega}_s \cdot \mathbf{h} \times \mathbf{e})\mathbf{h} \\
 h \left(\frac{d\mathbf{e}}{dt} \right)_{\text{qp}} &= \frac{\alpha_p}{(1-e^2)^2} \left[\frac{1}{2} \left(\frac{3}{h^2} (\boldsymbol{\Omega}_p \cdot \mathbf{h})^2 - \Omega_p^2 \right) \right. \\
 &\quad \left. + \frac{15 GM_s}{a^3} f_2(e^2)(1-e^2)^2 \right] (\mathbf{h} \times \mathbf{e}) \\
 &\quad + \frac{\alpha_p}{h^2(1-e^2)^2} (\boldsymbol{\Omega}_p \cdot \mathbf{h})(\boldsymbol{\Omega}_p \cdot \mathbf{h} \times \mathbf{e})\mathbf{h} \quad (16)
 \end{aligned}$$

$$h \left(\frac{d\mathbf{e}}{dt} \right)_{\text{GR}} = \frac{3 G(M_s + M_p)n}{ac^2(1-e^2)} (\mathbf{h} \times \mathbf{e}), \quad (17)$$

where \mathbf{n} is a unit vector that is perpendicular to the plane of the outer body's orbit (not to be confused with n and n_o , which are the angular frequencies of the inner and outer orbits), and

$$\alpha_s = \frac{R_s^5 k_s M_p}{2\mu n a^5} \quad \alpha_p = \frac{R_p^5 k_p M_s}{2\mu n a^5} \quad (18)$$

$$C_b = \frac{M_o}{M_s + M_p + M_o} \frac{n_o^2}{n} \frac{1}{4(1-e^2)^{1/2}(1-e_o^2)^{3/2}}. \quad (19)$$

In equation (18), k_s and k_p are the inner star and planet's tidal love numbers.

2.1 Octupole terms

It now appears that expanding the equations only to quadrupole order may not be appropriate for many systems (Naoz et al. 2011; Naoz, Farr & Rasio 2012), so we have also included the octupole terms. This allows us to consider situations in which the outer body's mass is comparable to that of the inner planet, and to consider situations in which the outer orbit is eccentric.

We are unable to write the octupole terms in a way that is regular at $e = 0$, so have implemented the form in (Mardling & Lin 2002). The octupole contributions are

$$\begin{aligned}
 \left(\frac{d\mathbf{h}}{dt} \right)_{\text{oct}} &= \frac{G(M_s + M_p)}{a} \left(\frac{M_o}{M_s + M_p} \right) \left(\frac{M_s - M_p}{M_s + M_p} \right) \\
 &\quad \times \left(\frac{a}{R} \right)^4 \frac{15e}{16} \left\{ 10(1-e^2)\hat{R}_1\hat{R}_2\hat{R}_3\hat{\mathbf{e}} \right. \\
 &\quad \left. + \left[(4+3e^2)\hat{R}_3 - 5(3+4e^2)\hat{R}_1^2\hat{R}_3 \right. \right. \\
 &\quad \left. \left. - 5(1-e^2)\hat{R}_2^2\hat{R}_3 \right] \hat{\mathbf{q}} \right. \\
 &\quad \left. - \left[(4+3e^2)\hat{R}_2 - 5(1+6e^2)\hat{R}_1^2\hat{R}_2 \right. \right. \\
 &\quad \left. \left. - 5(1-e^2)\hat{R}_2^3 \right] \hat{\mathbf{h}} \right\} \quad (20)
 \end{aligned}$$

$$\begin{aligned}
 \left(\frac{d\mathbf{e}}{dt} \right)_{\text{oct}} &= -n \left(\frac{M_o}{M_s + M_p} \right) \left(\frac{M_s - M_p}{M_s + M_p} \right) \\
 &\quad \times \left(\frac{a}{R} \right)^4 \sqrt{1-e^2} \frac{15}{16} \left\{ \left[-(4+3e^2)\hat{R}_2^2 \right. \right.
 \end{aligned}$$

$$\begin{aligned}
 &\quad \left. + (5+6e^2)\hat{R}_1^2\hat{R}_2 + 5(1-e^2)\hat{R}_3^3 \right] \hat{\mathbf{e}} \\
 &\quad + \left[(4+3e^2)\hat{R}_1 - 5(1-3e^2)\hat{R}_1\hat{R}_2^2 \right. \\
 &\quad \left. - 5(1+4e^2)\hat{R}_1^3 \right] \hat{\mathbf{q}} \\
 &\quad \left. + 10e^2\hat{R}_1\hat{R}_2\hat{R}_3\hat{\mathbf{h}} \right\}, \quad (21)
 \end{aligned}$$

where \mathbf{R} is the coordinate of the outer body, and the coordinate frame is defined by the basis vectors $(\hat{\mathbf{e}}, \hat{\mathbf{q}}, \hat{\mathbf{h}})$, with $\hat{\mathbf{q}} = \hat{\mathbf{h}} \times \hat{\mathbf{e}}$. The other unit vectors above are $\hat{R}_1 = \hat{\mathbf{R}} \cdot \hat{\mathbf{e}}$, $\hat{R}_2 = \hat{\mathbf{R}} \cdot \hat{\mathbf{q}}$, $\hat{R}_3 = \hat{\mathbf{R}} \cdot \hat{\mathbf{h}}$.

2.2 Integrating the outer orbit

The octupole terms described above need the coordinate of the outer body, which we determine by solving for the eccentric anomaly, E . This can be done by iterating the following equations until dE is below a threshold (we use 10^{-12})

$$\begin{aligned}
 dE &= \frac{-(E - e_o \sin E - l)}{1 - e_o \cos E} \\
 E &= E + dE, \quad (22)
 \end{aligned}$$

where l is the mean anomaly [$l = n_o(t - P)$], with P the orbital period and t the time since the completion of the last full orbit of the outer body. In all of our simulations, we fix the outer body to lie in the xy plane and so its co-ordinates are then

$$\begin{aligned}
 R_x &= a_o(\cos E - e_o) \\
 R_y &= a_o\sqrt{1-e_o^2} \sin E \\
 R_z &= 0, \quad (23)
 \end{aligned}$$

where a_o and e_o are the semimajor axis and eccentricity of the outer orbit. In this work, we neglect perturbations on the outer orbit.

2.3 Stellar wind

Without a stellar wind, or with a very weak stellar wind, it is possible that tidal interactions between the star and planet can result in the planet being trapped in a close orbit (Dobbs-Dixon, Lin & Mardling 2004). Most stars, however, have winds that continue to remove angular momentum, and so once tidal interactions become significant, we would typically expect the planet to continue spiralling in towards the central star. We implement here a very simple magnetic braking form for the stellar wind (Weber & Davis 1967; Kawaler 1988; Collier Cameron & Jianke 1994) so that in the unsaturated regime, the stellar wind term is

$$\dot{\Omega}_{\text{swind}} = -\kappa_w \Omega_s^3, \quad (24)$$

where κ_w is the braking efficiency coefficient. In the saturated regime (when $\Omega_s > \tilde{\Omega}$) this becomes

$$\dot{\Omega}_{\text{swind}} = -\kappa_w \Omega_s^2 \tilde{\Omega}. \quad (25)$$

The braking efficiency coefficient, κ_w , is set so that the stellar rotation period matches that expected for the star being considered, and $\tilde{\Omega}$ is set to be $14\Omega_{\odot}$. The vector associated with the stellar wind is always set so as to point in to opposite direction to that of the spin of the planet host star.

2.4 Putting it together

Ultimately we want to evolve the angular momentum, h , and eccentricity, e , of the inner orbit, and the spins of the planet and its host star, Ω_p and Ω_s . The evolution of the stellar spin is determined by combining the stellar wind equations (equations 24 and 25 with equation 3). The evolution of the spins of the star and planet (equation 4), both depend on the tidal evolution of the orbital angular momentum (equation 1).

To evolve the angular momentum of the inner orbit, we need to add the contributions from tides (equation 1), perturbations from an outer body expanded to quadrupole and octupole order (equations 13 and 20), and perturbations from distortions of the inner star and planet (equation 14). Similarly to evolve the eccentricity of the inner orbit, we combine the contributions from tides (equation 2), perturbations from an outer body expanded to quadrupole and octupole order (equations 15 and 21), perturbations from distortions of the inner star and planet (equation 16) and GR apsidal precession (equation 17).

2.5 Some basic tests

Since this is a new code, we ran a few comparison tests to check that it was working properly. The first was that introduced by Wu & Murray (2003). It comprises a $1.1 M_\odot$ star with a $7.8 M_{\text{Jup}}$ planetary companion, the star having a radius of $1R_\odot$ and the planet having a radius the same as that of Jupiter. The initial stellar and planetary spin periods are, respectively, 20 d and 10 h. The inner system's orbit has a semimajor axis of $a = 5.0$ au, and eccentricity $e = 0.1$, the tidal love numbers are $k_s = 0.028$ and $k_p = 0.51$, and the tidal dissipation quality factors are $Q'_s = 5.35 \times 10^7$ and $Q'_p = 5.88 \times 10^5$. The system also has a $1.1 M_\odot$ companion with $a_o = 1000$ au, $e_o = 0.5$ and with an orbital plane inclined at $85:6$ to that of the plane of the inner orbit.

Fig. 1 shows the time evolution of the semimajor axis (dashed line) and periaps ($a(1 - e)$ – solid line) of the system described above, and appears the same as that in Fabrycky & Tremaine (2007), who also performed this test. It is not quite the same as in Wu & Murray (2003), but we can match their result if we remove the apsidal precession due to the spin and tidal bulges of the planet (which can require very short timesteps and, hence, long integration times).

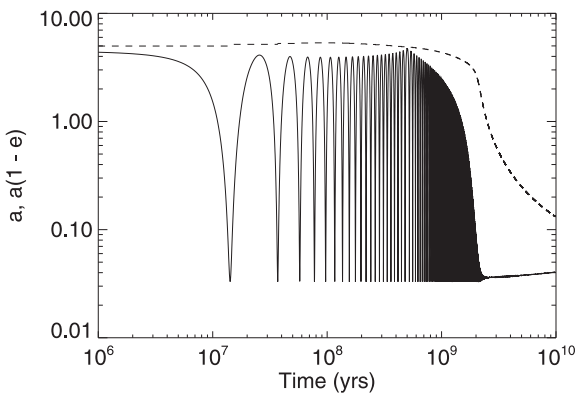


Figure 1. A figure showing the evolution of the semimajor axis (a – solid line) and the periaps ($a(1 - e)$ – dashed line) using initial conditions the same as those in Wu & Murray (2003). This was a code test that was also carried out by Fabrycky & Tremaine (2007), and our results appear to match theirs. It does not quite match Wu & Murray (2003) but we can match their results if we ignore the term representing the apsidal precession due to the spin and tidal bulges of the planet.

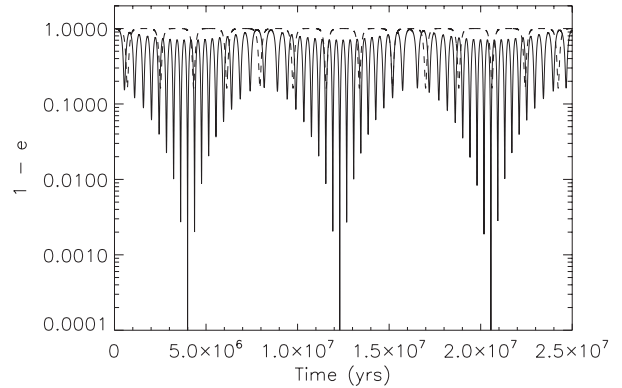


Figure 2. The evolution of $1 - e$ for a system with the same parameters as those used by Naoz et al. (2013) and described here in the text. The solid line shows the evolution when the octupole terms are included and it matches that of Naoz et al. (2013). The dashed line shows how the system would evolve in the absence of the octupole terms.

The second test was primarily to check that the octupole terms had been properly implemented. In this test, taken from Naoz et al. (2013), we ignore the tidal evolution terms, the terms associated with the distortion of the inner star and planet due to their tidal bulges, and the effect of GR apsidal precession. The system consists of an inner star of mass $1 M_\odot$, a companion planet with mass $1 M_{\text{Jup}}$, and an outer planet with mass $1 M_\odot$. The inner orbit has a semimajor axis of $a = 6$ au and eccentricity of $e = 0.001$. The outer orbit has a semimajor axis of $a_o = 100$ au, an eccentricity of $e_o = 0.6$ and is inclined at 65° to the plane of the inner orbit. The argument of pericentre of the inner orbit is also set, initially, to 45° with the outer one set to zero.

Fig. 2 shows the time evolution of $1 - e$ for the system described above. The result appears identical to that in Naoz et al. (2013). The dotted line also shows how the system would evolve in the absence of the octupole terms.

3 BASIC SETUP

The system we want to consider specifically is Kepler-78 (Sanchis-Ojeda et al. 2013). The companion planet, with a mass of $M_p = 1.86 M_\oplus$ and radius of $R_p = 1.173 R_\oplus$, is Earth-sized and has an Earth-like density ($\rho = 5.57 \text{ g cm}^{-3}$) (Howard et al. 2013; Pepe et al. 2013). The host star has a mass of $M_s = 0.81 M_\odot$ and radius $R_s = 0.737 M_\odot$, and the planet has an orbit that is circular ($e = 0$) and orbits at a distance $a = 0.0089$ au (giving an orbital period of 8.5 h).

The system is thought to have an age between 600 and 900 Myr (Sanchis-Ojeda et al. 2013), so here we run our initial simulations for 800 Myr. We set the stellar wind braking parameter to $\kappa_w = 10^{46}$, which gives a stellar rotation speed of between 11 and 12 d at $t = 800$ Myr, similar to that observed (Pepe et al. 2013). A star with a mass similar to that of Kepler-78, however, does not spin-down much in the first Gyr and so the stellar wind is probably not particularly important here. The tidal love numbers are set to $k_s = 0.028$ and $k_p = 0.51$, and we consider stellar tidal quality factors of $Q'_s = 5 \times 10^5$ and $Q'_p = 5 \times 10^6$. We will specify the tidal quality factor for the planet Q'_p , the planet's initial orbital properties and the properties of the outer body, when we discuss the results of the simulations.

4 RESULTS

Since we want to consider if Kozai–Lidov cycles could explain the properties of Kepler-78b, our models are set up in the following way. We assume we have a planet with a mass and radius the same as that of Kepler-78b with an initial semimajor axis between $a = 0.5$ and 2 au, with the semimajor axis chosen randomly in $\log a$. The initial eccentricity is set to be $e = 0.05$, chosen because we are assuming, here, that the planet has formed in a circumstellar disc in an almost circular orbit. We should acknowledge, however, that the initial eccentricity can have a significant impact on the evolution of co-planar systems (Li et al. 2014) and, therefore, stress that our results only apply to systems in which the inner system has a low initial eccentricity.

We also assume that there is an outer companion with a mass randomly chosen to be uniform between $M_o = 0.1 M_\odot$ and $M_o = 1 M_\odot$, a semimajor axis chosen randomly in $\log a$, between $a_o = 40$ au and $a_o = 20\,000$ au, and a randomly chosen eccentricity between $e_o = 0$ and $e_o = 1$. We then fix the outer companion’s orbit to be in the xy plane and randomly orientate the inner orbit so that the mutual inclination, i , is isotropic (Wu, Murray & Ramsahai 2007). We also randomly orientate the longitude of the planet’s ascending node. By choosing such a high-mass companion, we are essentially in the test particle regime (Lithwick & Naoz 2011). Such companions will also produce a large maximum eccentricity (for the inner orbit) than lower mass companions (Teyssandier et al. 2013). As such, we might expect a reasonably large number of tidal disruption events (Naoz, Farr & Rasio 2012; Li et al. 2014; Petrovich 2015). As such, our results only apply to a situation where the companion is of stellar mass.

We also impose stability criteria (Mardling & Aarseth 2001; Lithwick & Naoz 2011; Naoz et al. 2013) and insist that

$$\frac{a}{a_o} \frac{e_o}{1 - e_o^2} < 0.1, \quad (26)$$

and that

$$\frac{a_o}{a} > 2.8 \left(1 + \frac{M_o}{M_s + M_p} \right)^{2/5} \frac{(1 + e_o)^{2/5}}{(1 - e_o)^{6/5}} \left(1 - \frac{0.3i}{180^\circ} \right). \quad (27)$$

Equation (26) ensures that we are in the regime where the quadrupole and octupole terms dominate, while equation (27), in which i is the mutual inclination of the two orbits, ensures that the triple system is long-term stable (Mardling & Aarseth 2001). Equation (27) is almost always satisfied for the initial conditions used here.

4.1 Initial results

The tidal quality factor for a terrestrial planet is thought to lie between $Q'_p = 10$ and $Q'_p = 500$ (Goldreich & Soter 1966). Since we are considering a young system in which the planet likely retains a lot of its initial internal heat, we assume a value at the top of this range ($Q'_p = 500$), and also a more extreme case where $Q'_p = 5000$ (Henning, O’Connell & Sasselov 2009). For the star, we assume tidal quality factors of $Q'_s = 5 \times 10^5$ and $Q'_s = 5 \times 10^6$, within the range expected for exoplanet host stars (Baraffe, Chabrier & Barman 2010; Brown et al. 2011). For each simulation we select the initial conditions as described above and evolve the system until $t = 800$ Myr, using a fourth-order Runge–Kutta integrator. We repeat this 10 000 times for each set of parameters, and the basic result is shown in Fig. 3. The top panel is for $Q'_p = 500$ and the bottom for $Q'_p = 5000$. The solid line in each figure is for $Q'_s = 5 \times 10^6$, the

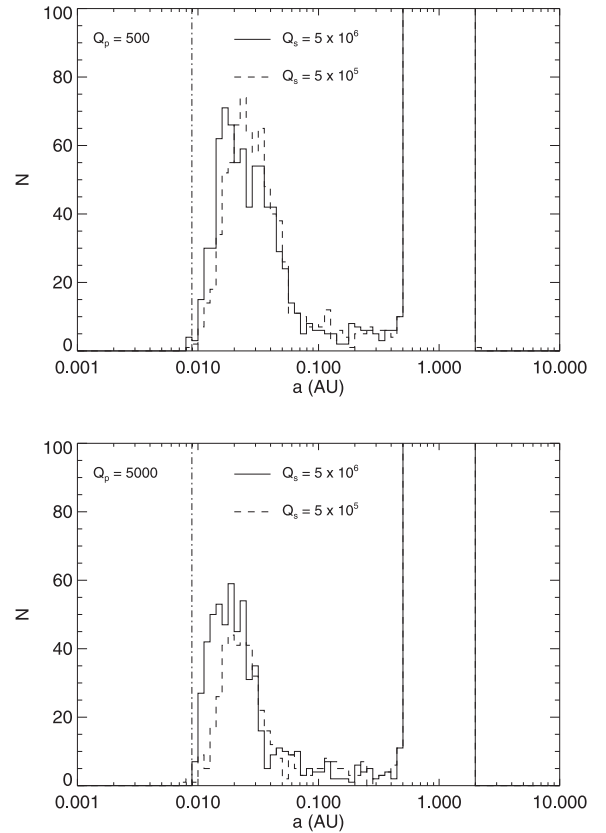


Figure 3. Histograms showing the final semimajor axes of the simulations with initial setup as described in the text and in which each simulation is stopped at $t = 800$ Myr. The top panel is for $Q'_p = 500$ and the bottom is $Q'_p = 5000$. The stellar tidal quality factors that we consider are $Q'_s = 5 \times 10^6$ (solid line) and $Q'_s = 5 \times 10^5$ (dashed line). We consider 10 000 systems in each case, with the planet starting with a between 0.5 and 2 au. After 800 Myr, there are between 10 and 4 planets surviving inside $a = 0.01$ au, depending on the values of Q'_p and Q'_s . The vertical dash-dotted line indicates the current semimajor axis of Kepler-78b. In each case, the number of planets still located between 0.5 and 2 au is very large, and their distribution extends well above the limits shown on the y -axis.

dashed line is for $Q'_s = 5 \times 10^5$, and the vertical dash-dotted line indicates the current semimajor axis of Kepler-78b. In each case, the number of planets still located between 0.5 and 2 au is very large and their distribution extends well above the limits shown on the y -axis.

From Fig. 3 it seems clear that it is possible for a planet to be perturbed into an orbit inside $a = 0.01$ au within 800 Myr. However, the numbers are typically small. For $Q'_p = 500$ it is 10 ($Q'_s = 5 \times 10^6$) and 4 ($Q'_s = 5 \times 10^5$), while for $Q'_p = 5000$ it is 7 and 4, respectively. Even though the number of planets surviving inside $a = 0.01$ au is small, in most cases, a much larger number reach their Roche limit [$a = R_p/0.462(M_s/M_p)^{1/3} = 0.0056$ au] (Faber, Rasio & Willems 2005) and are assumed to be tidally disrupted and destroyed. With the exception of the $Q'_p = 500$, $Q'_s = 5 \times 10^6$ simulation (in which the numbers were small), in excess of 100 – out of a sample of 10 000 – reached the Roche limit.

Given that a large numbers of planets do become tidally destroyed, it is useful to know for how long a planet might exist inside $a = 0.01$ au. Fig. 4 shows four single planet simulations, one for each combination of Q'_p and Q'_s , each of which is run until the planet reaches its Roche limit. The amount of time such a planet spends

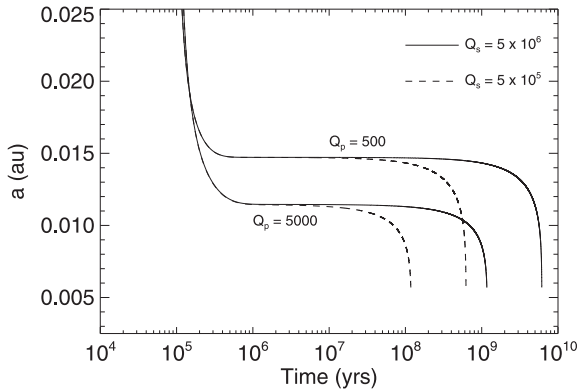


Figure 4. A set of single planet simulations, each with a different Q'_p or Q'_s value. In each case we have chosen initial conditions that would indeed perturb the planet into a close orbit, and have run each simulation until the planet reaches its Roche limit ($a = 0.0056$ au in this case). The time a planet spends inside 0.01 au before reaching its Roche limit depends primarily on the star's tidal quality factor and varies from 48 Myr ($Q'_s = 5 \times 10^5$) to 480 Myr ($Q'_s = 5 \times 10^6$).

inside $a = 0.01$ au depends, primarily, on the star's tidal quality factor. For $Q'_s = 5 \times 10^6$, the planet reaches the Roche limit in 480 Myr, while for $Q'_s = 5 \times 10^5$ it takes 48 Myr. Therefore, it would seem that for reasonable estimates of the star's tidal quality factor, a planet such as Kepler-78b will only be detectable inside $a = 0.01$ au for a few hundred Myr at most.

Our initial results would therefore seem to suggest that it is possible for an outer companion to perturb a planet like Kepler-78b into a very close orbit ($a < 0.01$ au) within the age of the system (~ 800 Myr). However, the numbers are small, with at most 10 out of 10 000 surviving inside $a = 0.01$ au at $t = 800$ Myr.

4.2 Age of the system

The previous simulations only considered the likelihood of a system with an age similar to that of Kepler-78, having a planetary companion with orbital properties similar to that of Kepler-78b. The results suggest it is possible, but probably rare. Additionally, the age distribution of a sample of 950 *Kepler* object of interest host stars (Walkowicz & Basri 2013) suggests that about 10 percent have ages less than 1 Gyr. This is also probably biased towards younger stars because of the way in which the sample was selected. Given that about 40 percent of these would have stellar companions (Raghavan et al. 2010) would further reduce the likelihood of actually observing a Kepler-78b-type system.

To investigate how our results might depend on the age of the system, we reran our simulations with the same set of parameters as described above, but allowed the age of the star to vary, uniformly, from 500 Myr, to 2 Gyr. The resulting histograms are shown in Fig. 5 and are very similar to those in Fig. 3. There is a slight increase in the number surviving inside $a = 0.01$ au for $Q'_s = 5 \times 10^6$. In these runs there were 17 and 16 for $Q'_p = 500$ and $Q'_p = 5000$ respectively, compared to 10 and 7 when the age of the system was fixed at $t = 800$ Myr. For $Q'_s = 5 \times 10^5$, the numbers are similar to the runs with the age fixed at $t = 800$ Myr.

To further see the influence of the age of the system, we plot in Fig. 6 the final semimajor axis of the planet against age of the system, for all those systems in which planets end up inside 0.05 au. We only show, however, the results for $Q'_p = 5000$, $Q'_s = 5 \times 10^6$ as that produced the largest number of surviving planets inside

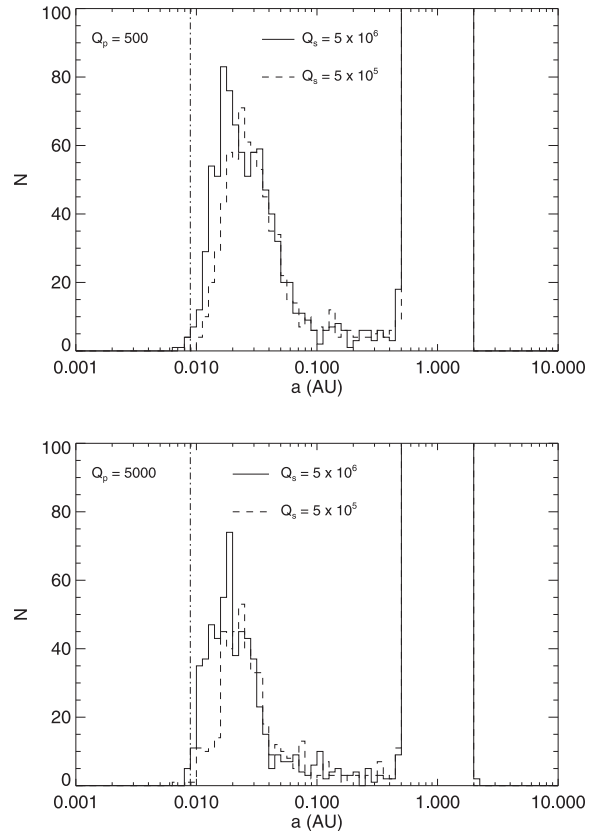


Figure 5. Histograms showing the final semimajor axes for the simulations with initial setup as described in the text and in which the age of each system is randomly chosen to be between 500 Myr and 2 Gyr. The top panel is for $Q'_p = 500$ and the bottom is $Q'_p = 5000$. The stellar tidal quality factors that we consider are $Q'_s = 5 \times 10^6$ (solid line) and $Q'_s = 5 \times 10^5$ (dashed line). We consider 10 000 system in each case, and the planets start with a between 0.5 and 2 au. In each case, the number of planets still located between 0.5 and 2 au is very large, and their distribution extends well above the limits shown on the y-axis. Depending on the values of Q'_p and Q'_s , there are between 17 and 6 planets surviving inside $a = 0.01$ au.

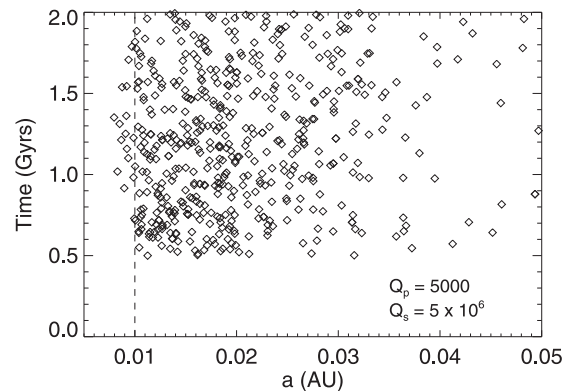


Figure 6. Figure showing the final semimajor axes for those planets that end up with $a < 0.05$ au, plotted against the age of the system. This simulations each considered 10 000 systems in which the outer perturber was assumed to have a semimajor axis distribution that extended to $a_o = 20\,000$ au. It is clear that it is possible for a system with an age similar to that of Kepler-78 to have a planet inside 0.01 au, but it is more likely for systems older than 1 Gyr, than for those with ages below 1 Gyr.

$a = 0.01$ au. The first thing to note is that it appears more likely to detect such a planet for systems older than 1 Gyr (Kepler-78 has an age of between 600 and 900 Myr). However, Fig. 6 does show four systems with an age < 1 Gyr, and with a planet inside $a = 0.01$ au.

Walkowicz & Basri (2013) also suggest that maybe 20 per cent of the *Kepler* targets have ages less than 2 Gyr. *Kepler* observed about 150 000 stars (Borucki et al. 2010), which suggests maybe as many as 30 000 could have ages less than 2 Gyr. Candidates as small as Kepler-78b, however, are typically found around quieter – and therefore older – stars. *Kepler* is therefore incomplete for stars with high Combined Differential Photometric Precision (Batalha et al. 2013; Christiansen et al. 2013) and so the number of such planets is likely an underestimate. In the scenario shown in Fig. 6, 17 – out of 10 000 – survive inside $a = 0.01$ au. If we assume that 40 per cent of those stars have stellar companions (Raghavan et al. 2010), and that all of those stars could host terrestrial planets (Greaves & Rice 2011; Cassan et al. 2012), then we might expect as many as 20 of the 30 000 *Kepler* targets, with ages below 2 Gyr, to host such an ultra-close-in planet. Of course, our other simulations suggest that the number surviving could be as low as two (depending on the tidal properties of the star and planet), but given that the chance of such a system transiting is actually quite high (46 per cent), observing such a system is still quite likely.

Similarly, if we consider only those systems with ages below 1 Gyr, Fig. 6 suggests that maybe as many as four out of 10 000 could survive inside $a = 0.01$ au. Repeating the calculation above suggests that maybe 4–5 stars with ages similar to that of Kepler-78 could host such a close-in planet. Again, given the high transit probability for such a close-in system, detecting a planet such as Kepler-78b becomes possible. Our results therefore suggest that it is possible for this process to have produced a planet like Kepler-78b. Of course, if Kepler-78 is closer in age to 600 Myr, than to 900 Myr, Fig. 6 suggests that it would become less likely.

4.3 Perturber properties

The results above suggest that it is possible for an outer perturber to drive a Kepler-78b-like planet into a close-in orbit within the age of Kepler-78. To see how the properties of the outer body influences the inner planet, we show – in Fig. 7 – how the final semimajor axis of the planet depends on the mass of the outer body. Again, we only shows results from the simulation with $Q'_p = 5000$

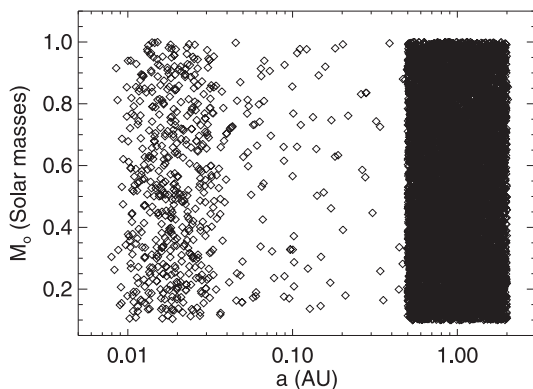


Figure 7. Figure showing the planet’s final semimajor axis plotted against the mass of the outer companion. There appears to be little dependence on companion mass. *Kepler* would probably have detected a companion with a mass in excess of $\sim 0.5 M_{\odot}$, but this figure does show that a low-mass companion ($M < 0.5 M_{\odot}$) could indeed have produced a system like Kepler-78b system.

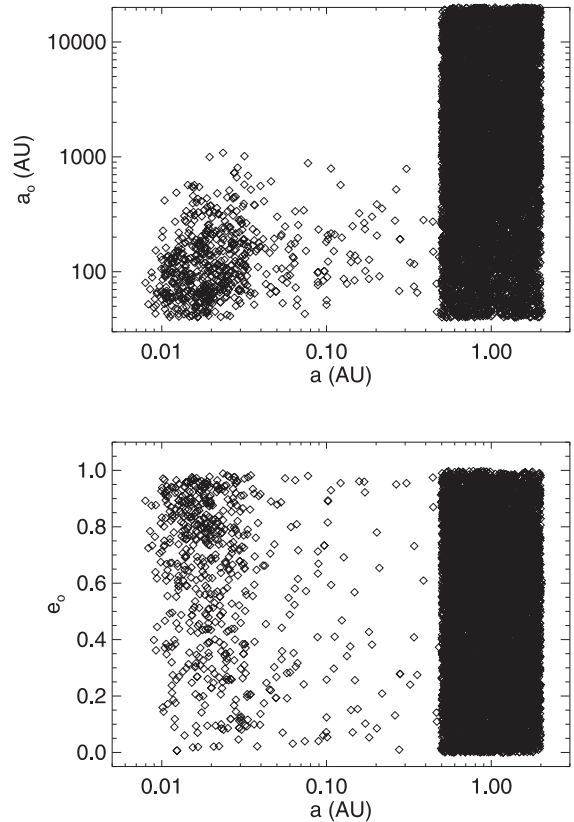


Figure 8. Figure showing how the orbital properties of the outer companion influences the final semimajor axis of the inner planet. The top panel shows that outer companions with smaller semimajor axes (a_o) are more likely to drive the planet to within $a = 0.01$ au. The bottom panel shows that outer companions with large eccentricities are more likely to perturb inner planets into very-close-in orbits, but that it is still possible for outer perturbers with low eccentricities.

and $Q'_s = 5 \times 10^6$. Fig. 7 suggests that there is not a particularly strong mass dependence, consistent with our simulations essentially being in the test particle regime (Lithwick & Naoz 2011). However, Kepler-78, which has an apparent magnitude of $m_v = 12$, is not known to host a stellar companion. Since *Kepler* is sensitive down to an apparent magnitude of $m_v = 14$, that would suggest that if there is an undetected companion it would need to have a mass less than about $0.5 M_{\odot}$.

Fig. 8 shows how the final semimajor axis of the planet, a , depends on the orbital properties of the outer body. The top panel shows that it is more likely that the planet will end up close to the parent star, if the outer body is in a relatively close orbit ($a_o \sim < 100$ au). *Kepler*’s has a 4 arcsec pixel size, and so Fig. 7 does suggest that a sufficiently faint, non-variable companion – that could have perturbed a planet into a Kepler-78b-like orbit – could indeed have avoided detection. The bottom panel of Fig. 8 shows how the final semimajor axis of the planet depends on the eccentricity (e_o) of the outer body. It indicates that close-in orbits are a little more likely when the companion has a high eccentricity ($e > 0.4$) but are still possible for those with smaller eccentricities.

4.4 The pile-up inside 0.1 au

Figs 3 and 5 show a pile-up of planets inside $a = 0.1$ au, peaking at ~ 0.02 au. In our simulations, between 350 and 850 (between 3.5 and 8.5 per cent of the full sample of 10 000) had final semimajor

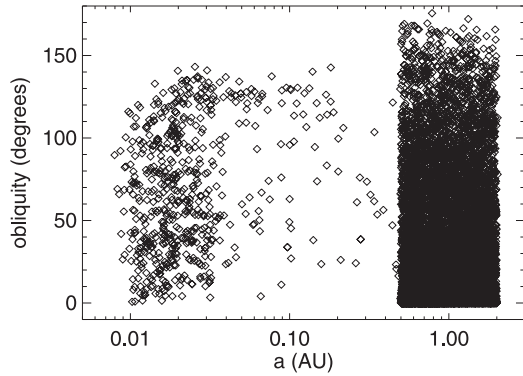


Figure 9. Figure showing the obliquity of the inner system. The inner system starts with the orbital angular momentum aligned with the spins of the central star and planet. The perturbation from the outer companion can, however, cause the inclination of the inner orbit to oscillate and those system that are tidally circularized can end up with a range of obliquities.

axes inside $a = 0.1$ au (and had not reached their Roche limit). If we assume that 40 per cent of the *Kepler* sample could have a binary companion (either primordial or through an exchange interaction) – and that most Sun-like stars have terrestrial-mass, planetary companions (Greaves & Rice 2011; Cassan et al. 2012) – then our results suggest that as much as 3 per cent of the *Kepler* sample might have planets that have been perturbed into close-in orbits, with a distribution that peaks at about 0.02 au. This is intriguingly similar to the suggestion in Sanchis-Ojeda et al. (2014) that about 1 in 200 *Kepler* stars hosts a planet with a period of 1 d or less.

4.5 Obliquity

An interesting aspect of the Kozai–Lidov process is that it can perturb a planet into an orbit that is inclined with respect to its initial plane and, hence, inclined with respect to the spin of the host star (Fabrycky & Tremaine 2007; Wu et al. 2007). We now have a number of close-in, ‘hot’ Jupiters that are on orbits inclined with respect to the spin of the host star (Hébrard et al. 2008; Triaud et al. 2010) and these are thought to be a consequence of Kozai–Lidov cycles. Fig. 9 shows the final angle (obliquity) between the angular momentum vector of the inner planet’s orbit and the spin of the central star, and shows that a wide range of obliquities are possible. All the systems initially have obliquities of zero (the angular momentum of the inner orbit is aligned with the spins of the parent star and planet) and Fig. 9 shows that those that are perturbed into an inner orbit can then be tidally circularized with a large range of obliquities, consistent with other similar studies (Fabrycky & Tremaine 2007; Naoz et al. 2012). Using the Rossiter–McLaughlin method to determine such a misalignment (e.g. Queloz et al. 2000) is probably not possible for such a low-mass planet, but it may be possible to do so using spot-crossing (Desert et al. 2011) or astro-seismology (Chaplin et al. 2013).

5 DISCUSSION AND CONCLUSIONS

We have considered, here, if systems like Kepler-78b (an Earth-like exoplanet with a very close-in orbit) could be due to a perturbation from an outer companion on an, initially, inclined orbit. To do this, we consider a system in which the star and planet have the same masses and radii as in the Kepler-78 system (Howard et al. 2013; Pepe et al. 2013; Sanchis-Ojeda et al. 2013), but in which the planet initially has an almost circular orbit with a semimajor axis between

0.5 and 2 au. The system is also assumed to have an outer companion with a semimajor axis between 40 and 20 000 au, with an orbital eccentricity that can be as high as $e = 1$ (but constrained by stability criteria) and that may be inclined with respect to the plane of the inner orbit.

We ran a suite of Monte Carlo simulations in which we randomly select the inner and outer systems semimajor axes, the eccentricity of the outer system, the mass of the outer companion and the mutual inclination of the two orbits. We ran two sets of simulations, one where each system was evolved for $t = 800$ Myr, similar to the expected age of the Kepler-78 system, and the other where the age of the system was randomly selected to be between 500 Myr and 2 Gyr. Our basic results are as follows.

(i) It is possible for a planet to be perturbed into an orbit similar to that of Kepler-78b around a star with an age (600–900 Myr) similar to that of Kepler-78. Out of a sample of 10 000, between 4 and 10 survive inside $a = 0.01$ au.

(ii) If we consider a broader age range, the likely binarity of the *Kepler* sample, and the size of the *Kepler* sample, our results suggest that as many as 20 of the *Kepler* targets with ages less than 2 Gyr could host a Kepler-78b-like planet. Additionally, we find that a system with an age similar to that of Kepler-78 could indeed have been found to host a Kepler-78b-like planet.

(iii) A planet such as Kepler-78b will, quite quickly, reach its Roche limit and be tidally destroyed. Our results suggest that such a planet would only survive inside $a = 0.01$ au for a few hundred Myr, at most. In the simulations here, typically in excess of 100, but no more than 300, (out of 10 000) reached their Roche limit and were assumed to be destroyed. This appears consistent with other work that has also suggested that this process could lead to the tidal destruction of perturbed planets (Naoz et al. 2012).

(iv) Given *Kepler*’s 4 arcsec pixel size and magnitude limit, it is possible that a faint, non-variable companion that could drive Kozai–Lidov cycles may have gone undetected. That the companion appears to need to be inside 100 au, means that it may be possible to detect the resulting radial velocity drift.

(v) If a planet such as Kepler-78b were perturbed into its current orbit through Kozai–Lidov cycles, we might expect the star’s rotation axis to be misaligned with respect to the planet’s orbit. Measuring the star’s obliquity is quite difficult, but could be possible using spot-crossing (Desert et al. 2011) or using astro-seismology (Chaplin et al. 2013).

(vi) Even though it appears possible that a system such as Kepler-78b could form in this way, it appears to be more likely for system older than 1 Gyr, than for systems younger than 1 Gyr.

Our basic results, therefore, suggest that such a process could operate, but there are some caveats. Although it is possible for a system with an age similar to that of Kepler-78 to host a planet like Kepler-78b, the numbers are small (we may expect the *Kepler* sample to host only a few such planets). Additionally it seems that it would have been more likely to have found such a planet in a slightly older system. These results, therefore, suggest that Kozai–Lidov cycles could have played a role in the evolution of Kepler-78b, but do not rule out that there could be an alternative explanation, such as planet–planet scattering (Rasio et al. 1996). This, however, may suffer from the similar issues, since the dominant constraint – given the relatively low age of Kepler-78 – is the tidal evolution time-scale. This constraint would probably also apply to the tidal downsizing hypothesis (Nayakshin 2010), in which a massive gas-giant planet formed in the outer parts of the system, migrates rapidly inwards and loses masses via tidal stripping. That, of course, leaves the

possibility that disc migration (Ward 1997) moved this planet into a very close orbit which has since evolved, through tidal interactions with the host star, into the orbit it inhabits today. Again, this would also involve tidal evolution once the disc has dispersed and so may also have a similar time-scale issue, unless disc migration can place the planet sufficiently close to the parent star so that it can then tidally evolve to where it is today.

Recent work by Sanchis-Ojeda et al. (2014) suggest that about 1 out of every 200 stars hosts an ultrashort-period (USP) planet (period of 1 d or less). Although we have focused on Kepler-78b here and found that few of our simulated systems have final periods as short as Kepler-78b (8.5 h), many more have periods of 1 d or less. The exact number depends on the chosen parameters, but it varies from ~ 100 to just over 300 (from a total sample of 10 000). Given that not all stars are binaries, this is intriguingly similar to the result in Sanchis-Ojeda et al. (2014). Similarly, our results suggest that such a process should lead to a pile-up of planets with a peak at about 0.02 au, again consistent with Sanchis-Ojeda et al. (2014), who find that the occurrence rate rises with period from 0.2 to 1 d. It may, however, be difficult to distinguish a pile-up due to Kozai–Lidov cycles from what is expected from scattering in multiplanet systems (Schlaufman et al. 2010). Sanchis-Ojeda et al. (2014) do, however, suggest that almost all USPs have companion planets with period $P < 50$ d, which may provide a constraint on the formation process for these USPs.

We should also acknowledge the possibility that our assumptions do not properly represent the possible initial conditions such a system could have. The initial distribution of the planet in semimajor axis space may be different to what we have assumed and the orbital properties of the outer perturber may also be different. Similarly, the tidal properties of the parent star and planet may differ from what we have assumed. However, we should at least acknowledge that even though our results suggest that Kozai–Lidov cycles will rarely produce a planet with properties similar to that of Kepler-78b, Kepler-78b is itself rare. In that sense our results could be seen as somewhat consistent with our knowledge of such planets, but that – alone – does not allow us to determine if it is likely that such a process did indeed play a role in the evolution of Kepler-78b.

ACKNOWLEDGEMENTS

The author acknowledges very useful discussions with Adrian Barker, Gordon Ogilvie, Douglas Heggie, Andrew Collier Cameron, Duncan Forgan and Eric Lopez. KR gratefully acknowledges support from STFC grant ST/J001422/1. The author would also like to thank the anonymous referee whose comments substantially improved this paper. The research leading to these results also received funding from the European Union Seventh Framework Programme (FP7/2007-2013) under grant agreement number 313014 (ETA-EARTH).

REFERENCES

Abt H. A., Willmarth D., 2006, *ApJS*, 162, 207
 Baraffe I., Chabrier G., Barman T., 2010, *Rep. Prog. Phys.*, 73, 016901
 Barker A. J., 2011, PhD thesis, Univ. Cambridge
 Barker A. J., Ogilvie G. I., 2009, *MNRAS*, 395, 2268
 Batalha N. M. et al., 2013, *ApJS*, 204, 24
 Bell K. R., Cassen P. M., Klahr H. H., Henning Th., 1997, *ApJ*, 486, 372
 Borucki W. J. et al., 2010, *Science*, 327, 977

Brown D. J. A., Collier Cameron A., Hall C., Hebb L., Smalley B., 2011, *MNRAS*, 415, 605
 Cassan A. et al., 2012, *Nature*, 481, 167
 Chaplin W. J. et al., 2013, *ApJ*, 766, 101
 Christiansen J. L. et al., 2013, *ApJS*, 207, 35
 Collier Cameron A., Jianke L., 1994, *MNRAS*, 269, 1099
 Cosentino R., Lovis C., Pepe F. et al., 2012, in McLean I. S., Ramsay S. K., Takami H., eds, *Proc. SPIE Conf. Ser. Vol. 8446, Ground-based and Airborne Instrumentation for Astronomy IV*. SPIE, Bellingham, p. 84461V
 Desert J.-M. et al., 2011, *ApJS*, 197, 14
 Dobbs-Dixon I., Lin D. N. C., Mardling R. A., 2004, *ApJ*, 610, 464
 Dressing C. D., Charbonneau D., 2013, *ApJ*, 767, 95
 Duquennoy A., Mayor M., 1991, *A&A*, 248, 485
 Eggleton P. P., Kiseleva L. G., 2001, *ApJ*, 562, 1012
 Faber J. A., Rasio F. A., Willems B., 2005, *Icarus*, 175, 248
 Fabrycky D., Tremaine S., 2007, *ApJ*, 669, 1298
 Ford E. B., Rasio F. A., 2006, *ApJ*, 638, L45
 Goldreich P., Soter S., 1966, *Icarus*, 5, 375
 Greaves J. S., Rice W. K. M., 2011, *MNRAS*, 412, L88
 Hébrard G. et al., 2008, *A&A*, 488, 763
 Henning W. G., O’Connell R. J., Sasselov D. D., 2009, *ApJ*, 707, 1000
 Howard A. et al., 2013, *Nature*, 503, 381
 Ida S., Lin D. N. C., 2008, *ApJ*, 673, 487
 Kawaler S. D., 1988, *ApJ*, 333, 236
 Kley W., Crida A., 2008, *A&A*, 487, L9
 Kozai Y., 1962, *AJ*, 67, 591
 Li G., Naoz S., Kocsis B., Loeb A., 2014, *ApJ*, 785, 116
 Lidov M. L., 1962, *Planet. Space Sci.*, 10, 719
 Lithwick Y., Naoz S., 2011, *ApJ*, 742, 94
 Mardling R. A., Aarseth S. J., 2001, *MNRAS*, 321, 398
 Mardling R. A., Lin D. N. C., 2002, *ApJ*, 573, 829
 Mordasins C., Alibert Y., Benz W., 2009, *A&A*, 501, 1139
 Naoz S., Farr W. M., Lithwick Y., Rasio F. A., Teysandier J., 2011, *Nature*, 473, 187
 Naoz S., Farr W. M., Rasio F. A., 2012, *ApJ*, 754, L36
 Naoz S., Farr W. M., Lithwick Y., Rasio F. A., Teysandier J., 2013, *MNRAS*, 431, 2155
 Nayakshin S., 2010, *MNRAS*, 408, L36
 Pepe F. et al., 2013, *Nature*, 503, 377
 Petigura E. A., Marcy G. W., Howard A. W., 2013, *ApJ*, 770, 69
 Petrovich C., 2015, *ApJ*, 799, 27
 Queloz D., Eggenberger A., Mayor M., Perrier C., Beuzit J. L., Naef D., Sivan J. P., Udry S., 2000, *A&A*, 369, L13
 Raghavan D. et al., 2010, *ApJS*, 190, 1
 Rasio F., Tout C. A., Lubow S. H., Livio M., 1996, *ApJ*, 470, 1187
 Sanchis-Ojeda R., Rappaport S., Winn J. N., Levine A., Kotsen M. C., Latham D. W., Buchhave L. A., 2013, *ApJ*, 774, 54
 Sanchis-Ojeda R., Rappaport S., Winn J. N., Knotson M. C., Levine A., Mellah I. E., 2014, *ApJ*, 787, 47
 Schlaufman K. C., Lin D. N. C., Ida S., 2010, *ApJ*, 724, L53
 Tanaka H., Takeuchi T., Ward W. R., 2002, *ApJ*, 565, 1257
 Teysandier J., Naoz S., Lizarraga I., Rasio F., 2013, *ApJ*, 779, 166
 Triaud A. H. M. J. et al., 2010, *A&A*, 524, A25
 Vogt S. et al., 1994, in Crawford D. L., Craine E. R., eds, *Proc. SPIE Conf. Ser. Vol. 2198, Instrumentation in Astronomy VIII*. SPIE, Bellingham, p. 362
 Walkowicz L. M., Basri G. S., 2013, *MNRAS*, 436, 1883
 Ward W. R., 1997, *Icarus*, 126, 261
 Weber E. J., Davis L., 1967, *ApJ*, 148, 217
 Wu Y., Murray N., 2003, *ApJ*, 589, 605
 Wu Y., Murray N. W., Ramsahai J. M., 2007, *ApJ*, 670, 820

This paper has been typeset from a $\text{\TeX}/\text{\LaTeX}$ file prepared by the author.